THE SPACE CHARGE EFFECT IN LOW ENERGY MAGNETIZED ELECTRON BEAMS

SAJINI WIJETHUNGA

CENTER FOR ACCELERATOR SCIENCE
OLD DOMINION UNIVERSITY, NORFOLK, VA

Jefferson Lab

Old Dominion University

U.S. Department of Energy | Office of Science

JSA

Outline

- Motivation
  - Magnetized electron cooler dynamics
- Magnetized source setup
- Characterization of the magnetized beam
  - Measurements and simulations
- Space charge
  - Space charge current limitation
- Characterization of the space charge effect in magnetized beam
  - Measurements and simulations
- Redesigning of the DC high voltage photogun
  - Existing gun design
  - Modified gun design
- GPT simulations with the modified photogun
- Summary
- To-do list

Motivation

Magnetized Electron cooling:

Luminosity (two Gaussian beams head on collision): $\mathcal{L} = \frac{N_e N_i f N_b}{4\pi\sigma_e\sigma_i}$

where, N_e, N_i number of particles per bunch, σ_e, σ_i beam sizes of the two colliding beams, f rep rate , N_b number of bunches.

- To achieve the small beam size (small transverse emittance and less momentum spread) ion beam must be cooled

Requirements of the electron beam for efficient cooling:

- High bunch charge
- Low beam temperature

} These features combine to enhance the collective interaction, such as space charge effect which can adversely affect the cooling process.

Ion beam cooling is much more efficient in the presence of a uniform magnetic field

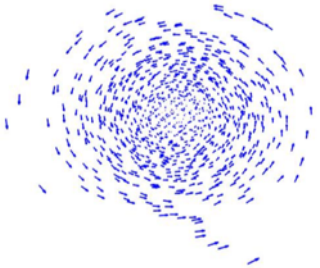

- The helical motion of an electron in a strong magnetic field increases electron-ion interaction time
- The cyclotron motion of the electrons due to the magnetic field suppresses electron-ion recombination

However, the radial fringe field at the entrance of the cooling solenoid exerts a large rotational motion on the electron beam that increases the beam size and thus the correlated emittance.

Magnetized Electron Cooler Dynamics

The magnetic field of the cathode solenoid is tuned to affect a zero-net rotation of the electron beam at the cooling solenoid.

Busch's theorem, canonical angular momentum

$$L = \gamma m_e r^2 \dot{\phi} + \frac{e}{2\pi}\psi = \gamma m_e r^2 \dot{\phi} \quad + \quad \frac{1}{2} e B_z r^2$$

is conserved.

Drift motion in between solenoids (larger radius)

Cyclotron motion (smaller radius)

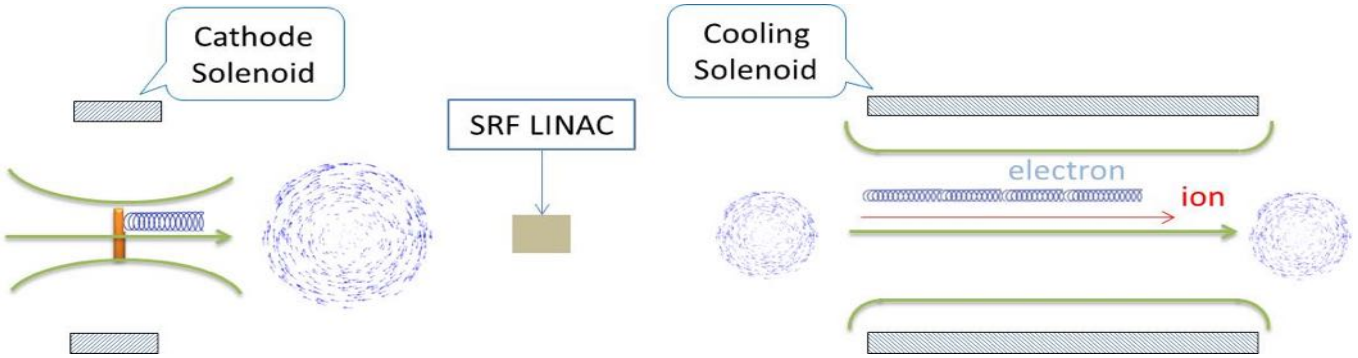

Electrons are born with transverse thermal momentum in magnetic field B_z each electron will have a helical cyclotron motion,
At the photocathode, $\dot{\phi}=0$

$$\langle L \rangle = \frac{eB_z a_o^2}{4}$$

Upon leaving the solenoid, $B_z = 0$
But due to the torque exerted in the transition region

$$\langle L \rangle = \gamma m_e \langle r \rangle^2 \dot{\phi}$$

Upon entering Cooling Solenoid

$$\frac{B_{cool}}{B_z} = \frac{a_0^2}{r_e^2}$$

Inside the cooling solenoid

$$\langle L \rangle = \frac{eB_{cool} r_e^2}{4}$$

Magnetized Source Schematic

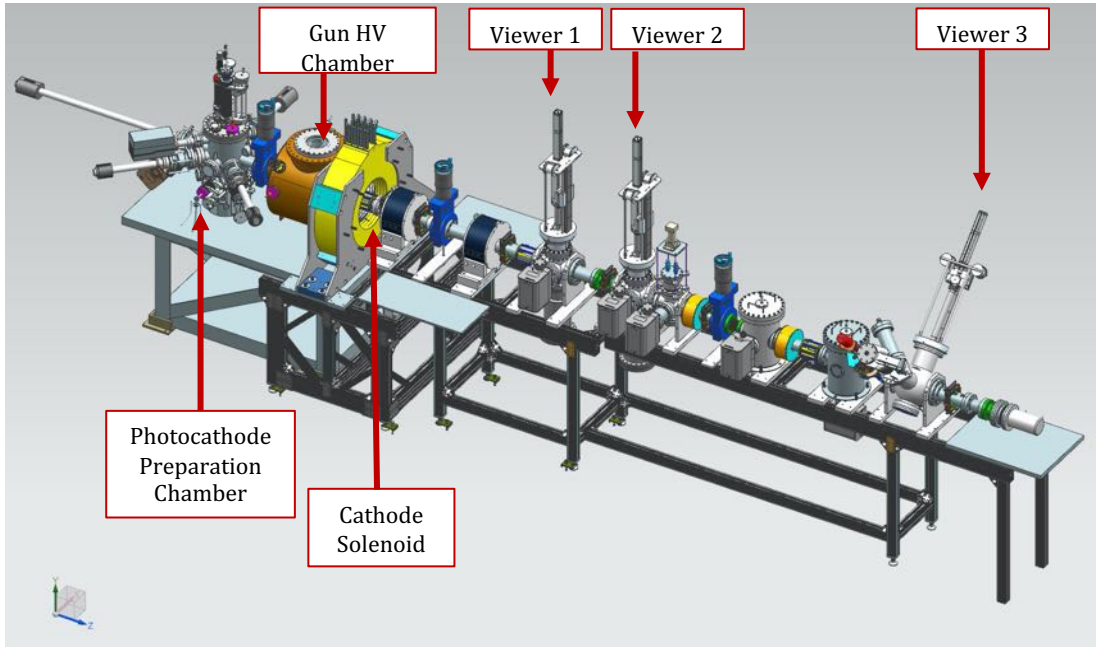

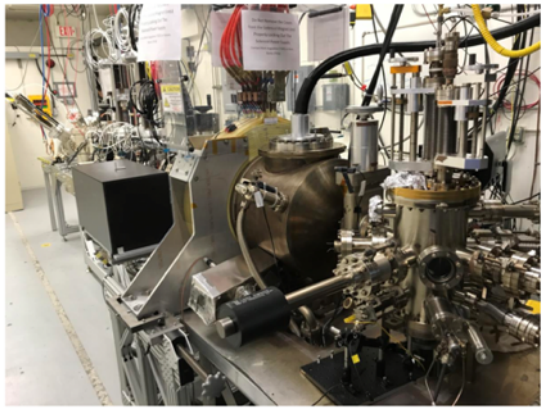

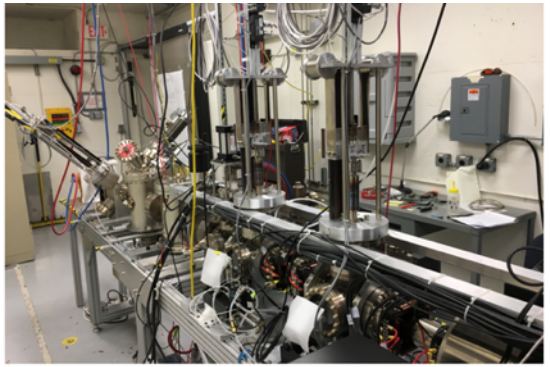

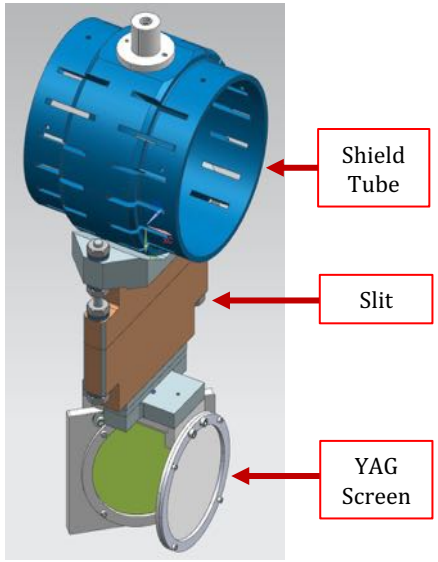

Use slit and viewer to measure rotation angle

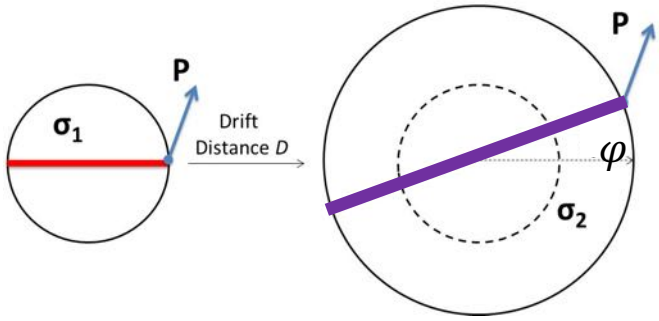

σ_i: beam size on i-th viewer
Φ : rotation angle

Photogun and Cathode Solenoid

Gun High Voltage Chamber

- Compact DC high voltage photogun with inverted insulator and spherical cathode electrode
- Operated at -300 kV

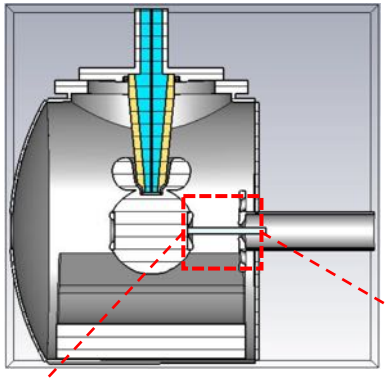

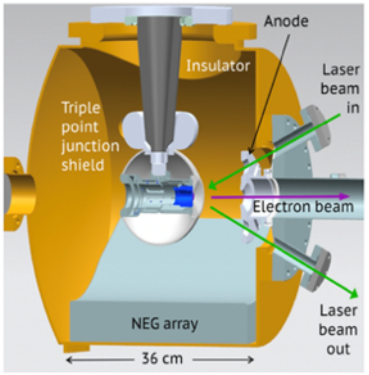

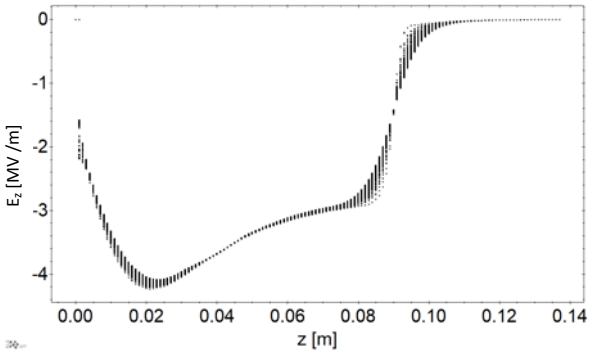

Cathode Solenoid

- Located 0.2 m away from the cathode
- Provides 1.5 kG to the cathode for a maximum of 400 A
- Field map is distorted due to the shield covers of the focusing solenoids next to it

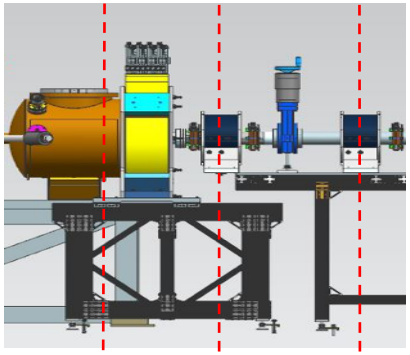

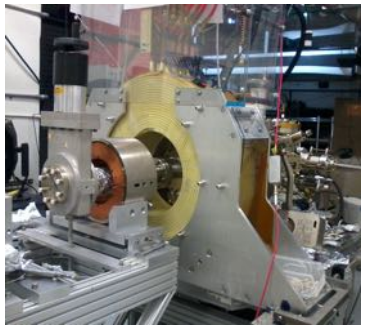

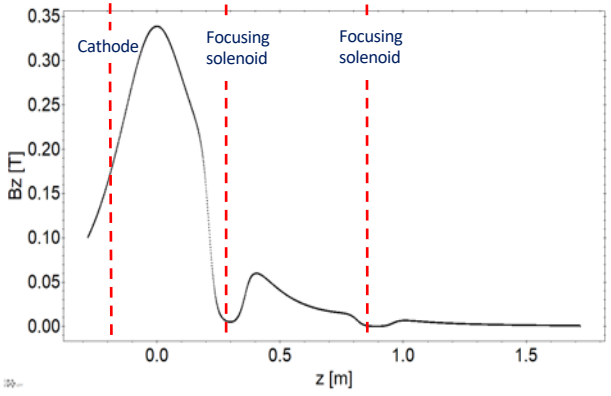

Photocathode and Laser

Bi-alkali Antimonide (K_2CsSb) Photocathode

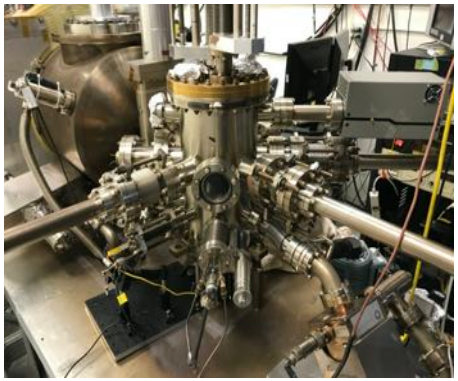

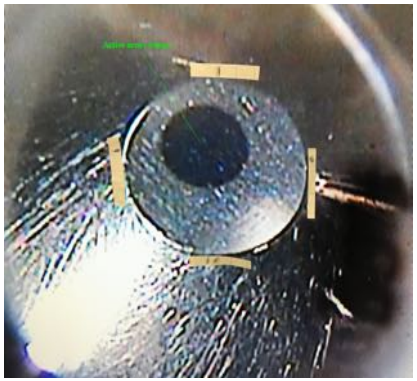

- Photocathode: GaAs substrate with 90 min deposition time of Sb layer
- Photocathode active area: 3 mm radius
- QE: 4-6% with 515 nm green laser

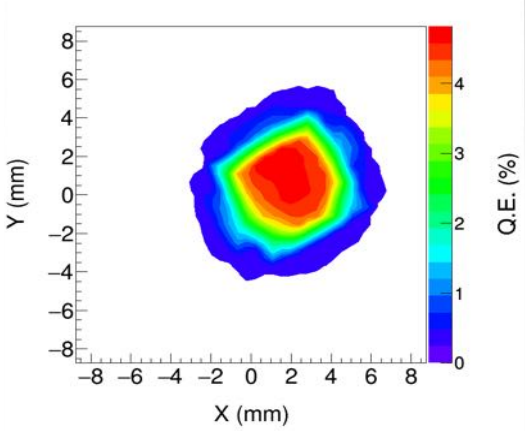

Laser

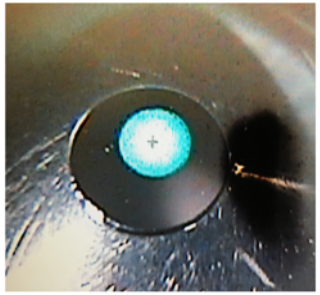

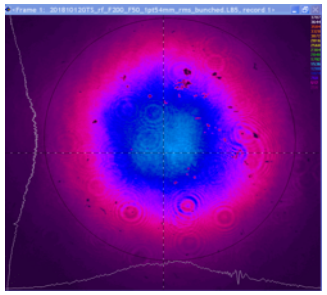

wavelength	515 nm
Pulse width	500 fs
Rep rate	Up to 50 kHz
Pulse energy	20 μJ

- Gaussian special and temporal profile
- Varied the laser size and pulse width using optical transport system with diffraction grating

Characterization of the magnetized beam

ASTRA Simulations

Mismatch oscillations

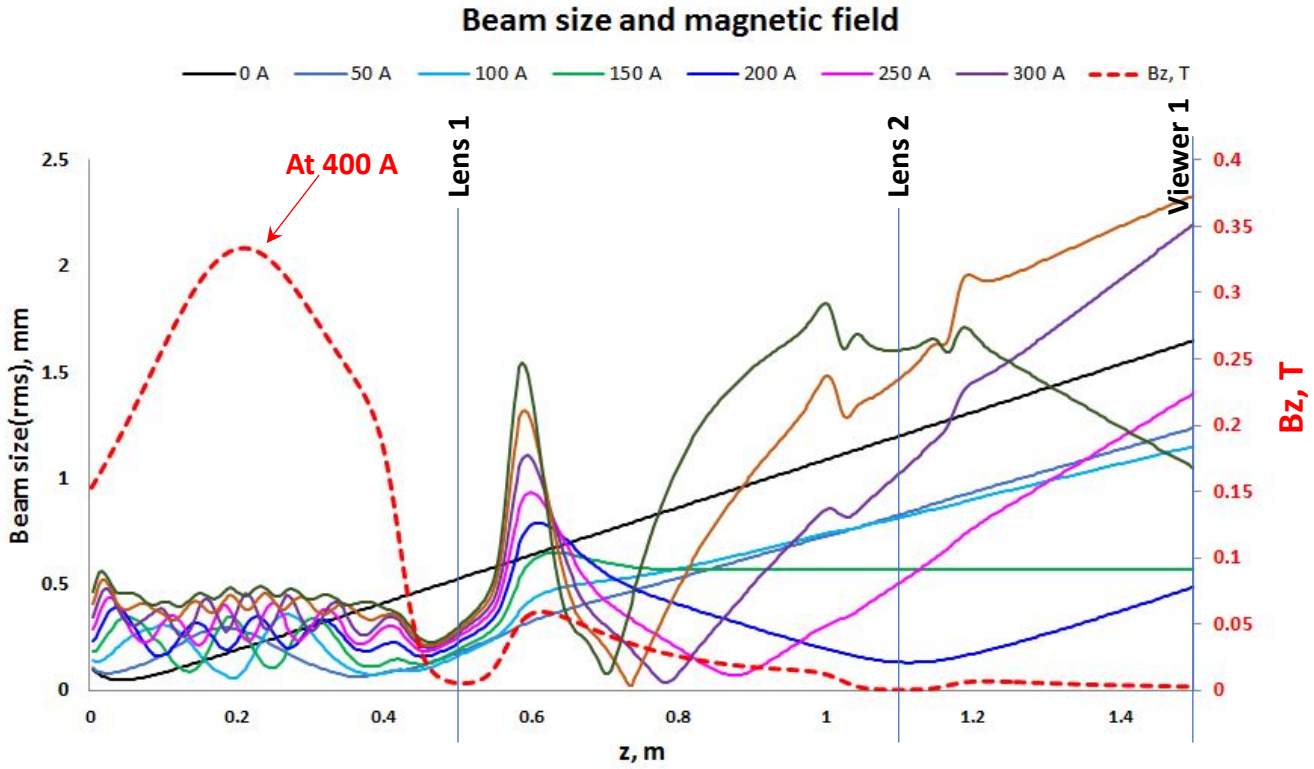

- The beam is converging and diverging with the gun solenoid strength which is known as mismatch oscillations
- This occurs due to our non-uniform magnetic field
- This also affects the beam size at exit of the gun solenoid field

Characterization of the magnetized beam

Beam size and Rotation angles

-300 kV, 0.3 mm (rms)

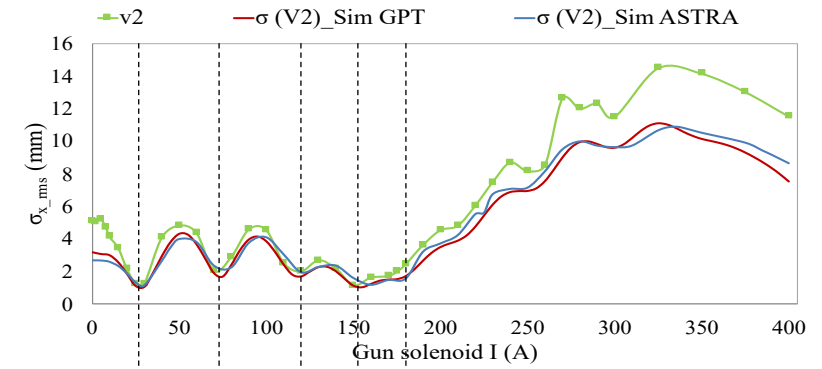

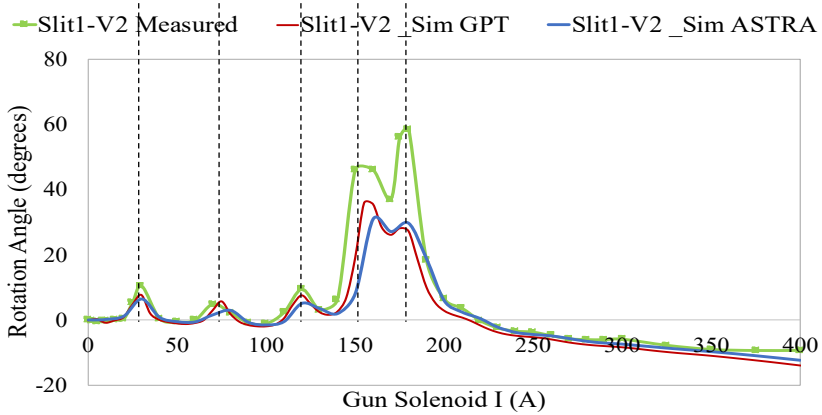

General formula to find the rotation angle φ :

$$\varphi_{rot} = tan^{-1}\left(\frac{\varphi\, z/v_z}{1 - z/f}\right)$$

φ_z -rotation from magnetization
z- drift length
v_z- velocity in z direction
f- focal length

When beam converging $\alpha > 0$ $\rightarrow \frac{\pi}{2} < \varphi_{rot} < \pi$

When beam is at waist $\alpha = 0$ $\rightarrow 0 < \varphi_{rot} < \frac{\pi}{2}$

When beam diverging $\alpha < 0$ $\rightarrow 0 < \varphi_{rot} < \frac{\pi}{2}$

Rotation angle variation of a diverging beam -180 A

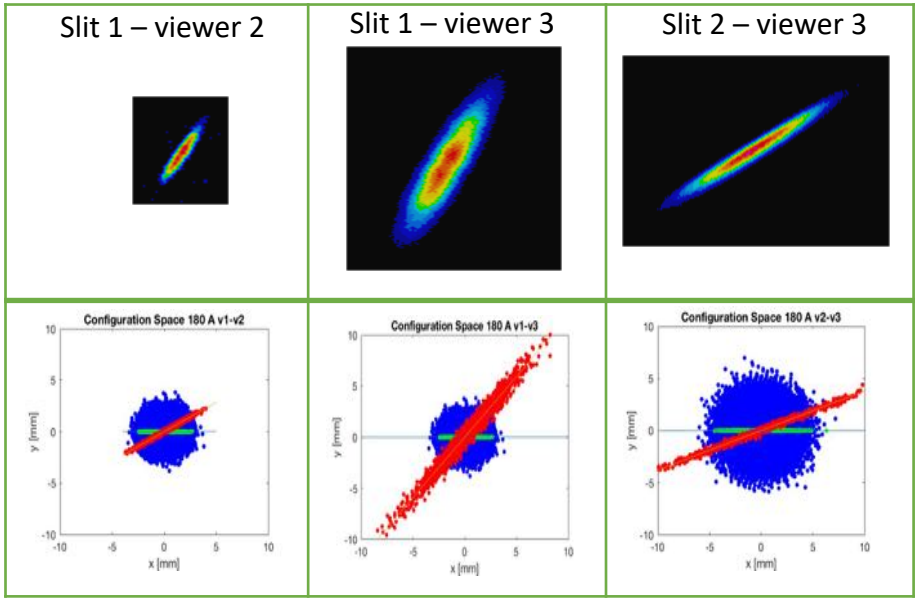

Rotation angle variation of a converging and diverging beam -100 A

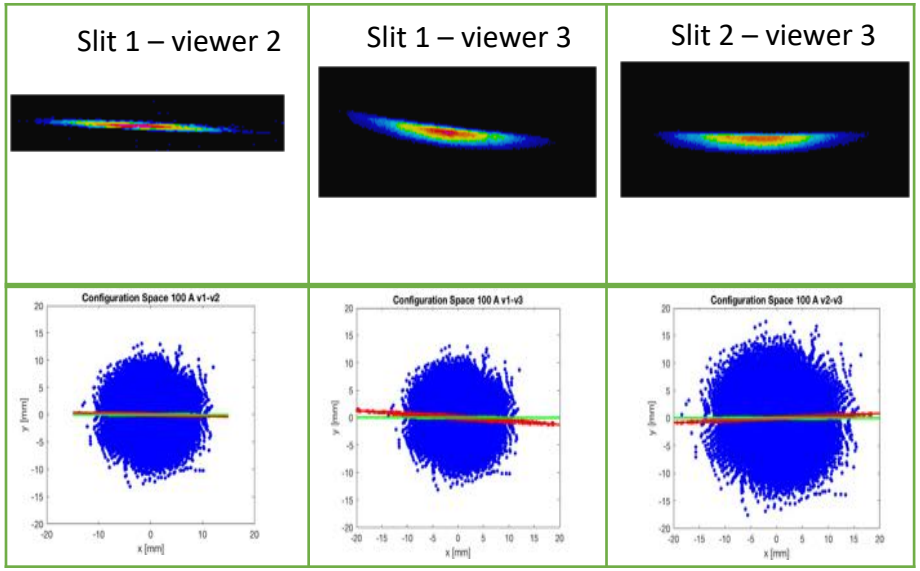

Emittance Compensation in a Magnetized Beam

- $\epsilon_{correlated}$ - Correlated - from the magnetization – large
- ϵ_0 - Uncorrelated – from the thermal energy at the cathode - small

$$\epsilon_{total} = \sqrt{{\epsilon_0}^2 + {\epsilon_{correlated}}^2}$$

Correlated emittance

Paraxial envelope equation for particle trajectory,

$$r_m'' + \frac{\gamma'}{\gamma\beta^2} r_m' + \frac{\gamma''}{2\gamma\beta^2} r_m + \left(\frac{qB}{2mc\beta\gamma}\right)^2 r_m - \left(\frac{p_\theta}{mc\beta\gamma}\right)^2 \frac{1}{{r_m}^3} - \left(\frac{\epsilon_0}{\beta\gamma}\right)^2 \frac{1}{{r_m}^3} - \frac{K}{r_m} = 0$$

Canonical angular momentum

Emittance variations

$$p_\theta = \gamma m r^2 \dot{\phi} + \frac{1}{2} e B_z {r_0}^2$$

Emittance term has the same r_m^{-3} dependence as the angular momentum term.

$$\left(\frac{p_\theta}{mc\beta\gamma}\right)^2 \frac{1}{{r_m}^3} = \left(\frac{\epsilon_0}{\beta\gamma}\right)^2 \frac{1}{{r_m}^3}$$

$$\epsilon_{correlated} = \frac{p_\theta}{mc} = \frac{e B_z {r_0}^2}{2mc}$$

B_z - Magnetic field at the cathode

r_0 - Beam size at the cathode

Magnetic field generates a canonical angular momentum that increases the total emittance.

Characterization of the magnetized beam

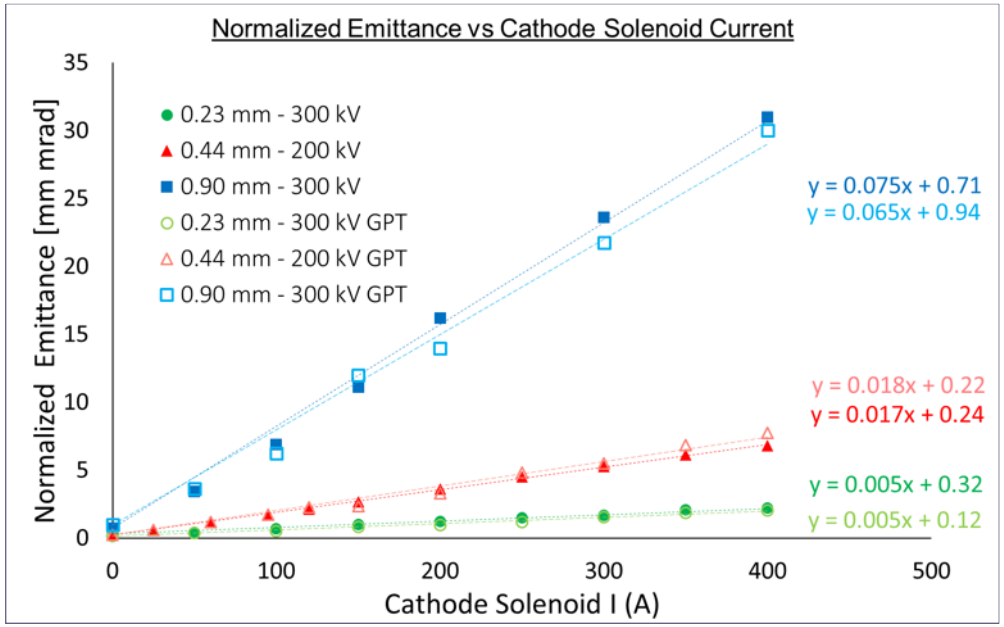

- Correlated emittance shows a linear dependence on the applied cathode magnetic field which consistent with the equation
- Significant beam loss at high magnetic field strengths made it difficult to measure accurately the desired drift emittance of 36 mm mrad for 400 A solenoid current, 0.9 mm laser size
- As predicted by theory, correlated emittance is clearly larger than the uncorrelated emittance.

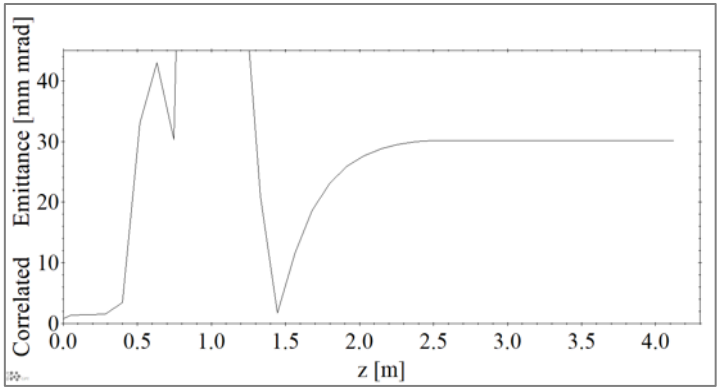

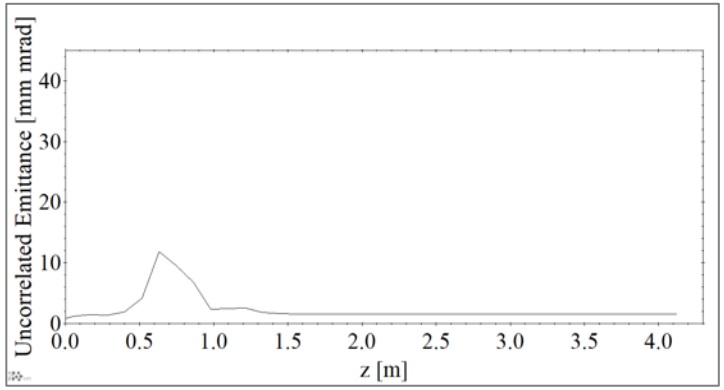

Correlated emittance: Huge emittance variation seen in between 0-2.5 m is due to the cathode solenoid field and 1st two focusing solenoid fields.

Uncorrelated emittance: When all the correlations are removed emittance should be small and a constant throughout the beamline. But the small bump seen in between 0.5-1m is due to the distorted magnetic field between the region.

Space Charge

Space charge forces

- Space charge is an accumulation of charges in a particular region
- Space charge forces are the Coulomb repulsive forces inside this region of charge accumulation
- Space charge forces can degrade the beam quality and cause instabilities, emittance growth, energy spread, halo formation, particle losses and even can set up an upper limit for the beam current

Space charge force acting on a charge inside the beam:

For a Gaussian distribution (r, z),

$$F_r(r,z) = \frac{q}{2\pi\epsilon_0\gamma^2}\frac{q_0}{\sqrt{2\pi}\,\sigma_z}e^{(-z^2/2{\sigma_z}^2)}\left[\frac{1-e^{(-r^2/2{\sigma_r}^2)}}{r}\right]$$

where q_0 bunch charge, σ_z and σ_r longitudinal and transverse rms beam sizes.

- For a non-magnetized electron beam: The bunch transverse dimension is small and the charge density is intense, hence the nonlinear space charge force can have huge effect during acceleration from low to higher energy and during the long drift, which would cause emittance growth beyond the specifications required for electron cooling.
- For a magnetized electron beam- The transverse size is set by the beam's correlated emittance which is controllable and much larger and thus the space charge effect is minimal.

Space charge current limitation

This charge accumulation forms a cloud of charges next to the cathode and it limits further emission of charges from the surface due to the space charge forces, is referred as the space charge current limit.

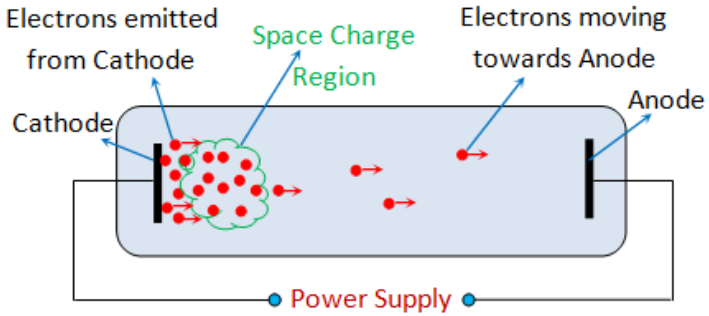

- Child and Langmuir first studied the maximum current density J that can be transported from an infinite planar cathode at zero potential to an infinite planar anode parallel to the cathode, when the initial velocity of electrons is zero, due to the space charge limitations,

$$J = \frac{4\epsilon_0}{9d^2}\sqrt{\frac{2e}{m}}V^{3/2}$$

where d distance between cathode and anode, V fixed potential.

- But most of the above assumptions are not the same for the practical situation.

- Hence, it can be used as a useful approximation.

Characterization of space charge effect in magnetized beam

- Increased the laser power at the cathode by keeping the other parameters constant and measured the average current at the end of the beamline for different solenoid strengths (0, 100, 200 A).
- Incident power can be related the extracted charge for a fixed QE value,

$$QE = \frac{hc}{\lambda e}\frac{I}{P} \times 100\% \quad \text{and} \quad I_{avg} = Q_{extracted}\, f$$

where, P (W) - incident laser power, I (mA) - measured average beam current, λ - laser wavelength (515 nm)

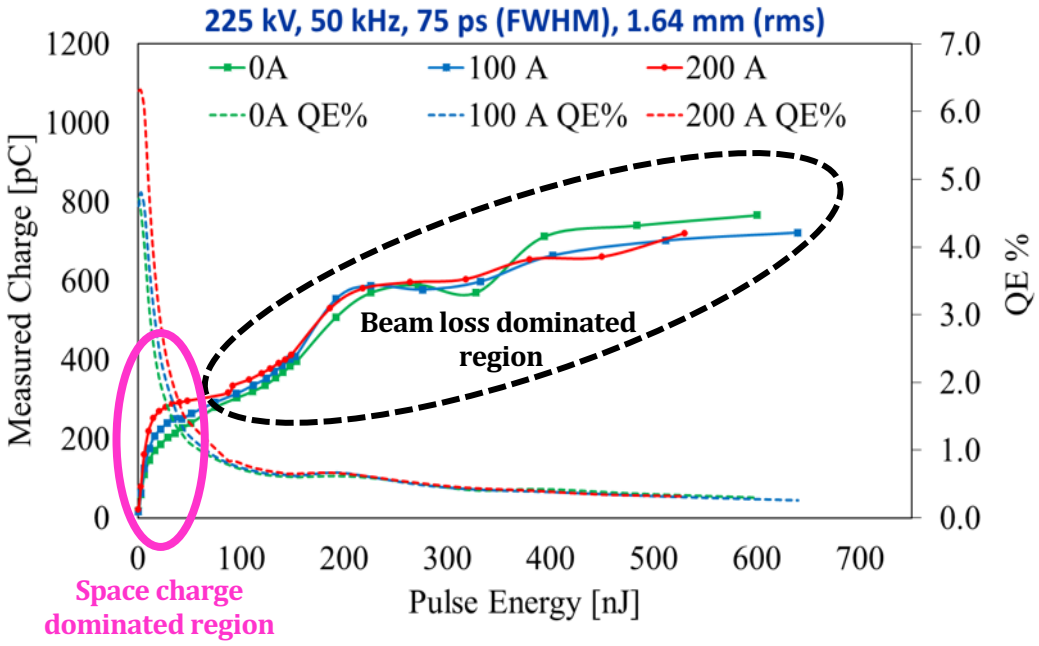

- QE falls rapidly with increasing laser power, implying that we have reached the space charge limitations immediately
- Space charge limitations were initiated as early as ~30 nJ
- The charge extracted from 300 pC to 700 pC seems coming from the edges of the Gaussian beam.

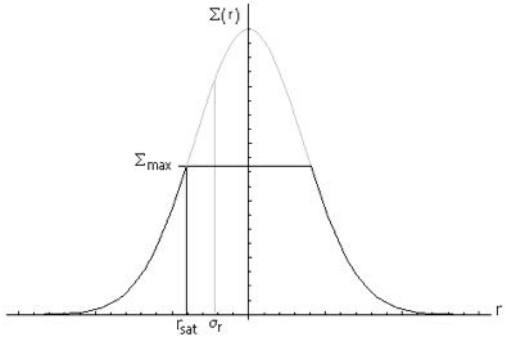

- Observed an increase in measured charge with cathode solenoid current only up to ~100 nJ
- The oscillatory behavior seen at higher pulse energies likely stems from beam loss
- Beam scraping due to limited beamline aperture and insufficient strength of the focusing solenoids prevent clean transport of beam to the dump for pulse energy >100 nJ

GPT Simulation vs. Measurements

- Simulation parameters:

Parameter	Value
Gun high voltage [kV]	-225
Magnetic field, B_z at the cathode [T] (0, 100, 200 A)	0, 0.038, 0.076
Mean Transverse Energy [eV]	0.130
Pulse width, Gaussian (FWHM) [ps]	75
Transverse laser spot size, Gaussian (rms) [mm]	1.64
Bunch charge [nC]	0.01 to 14.00
Horizontal offset of the laser [mm]	0
Vertical offset of the laser [mm]	1.70

- Optimized the steering magnets to center the beam
- Used field maps for the focusing solenoids
- Used profile product of laser intensity and QE distribution as the initial electron emission distribution

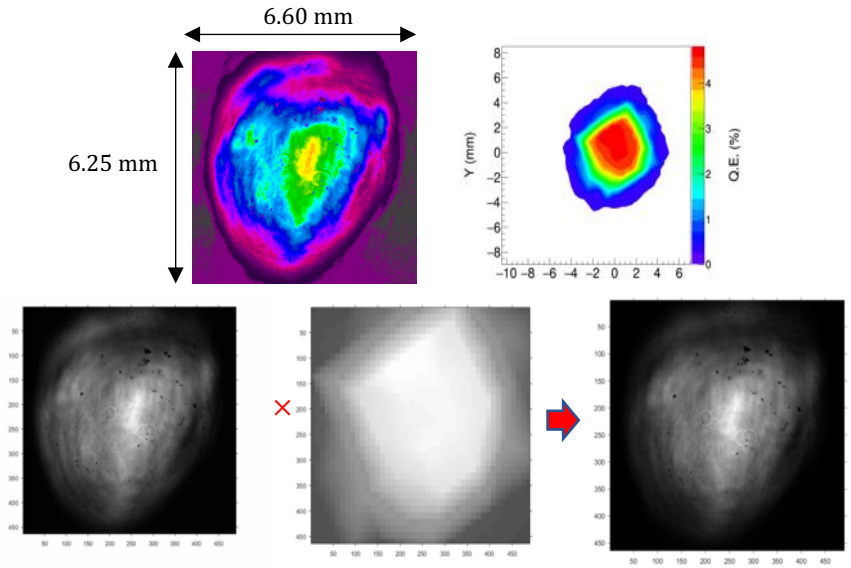

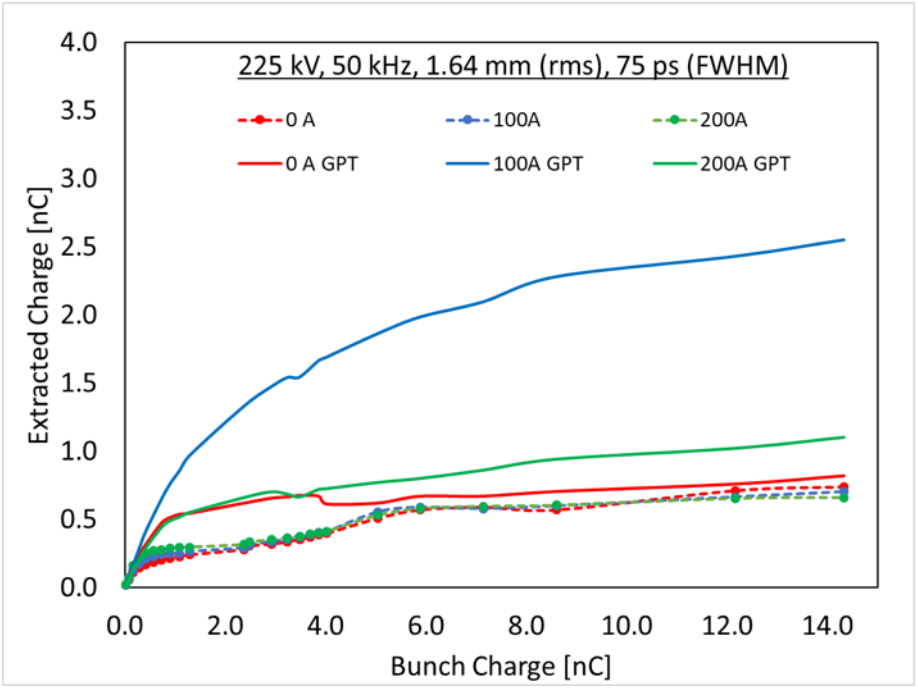

- GPT agrees fairly well with the measurements only for 0 A and 200 A cathode solenoid currents
- GPT extract more charge than measured for 100 A cathode solenoid current

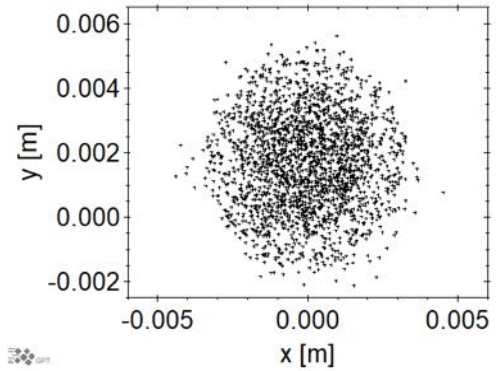

GPT Simulations Cont'd

Beam Trajectories

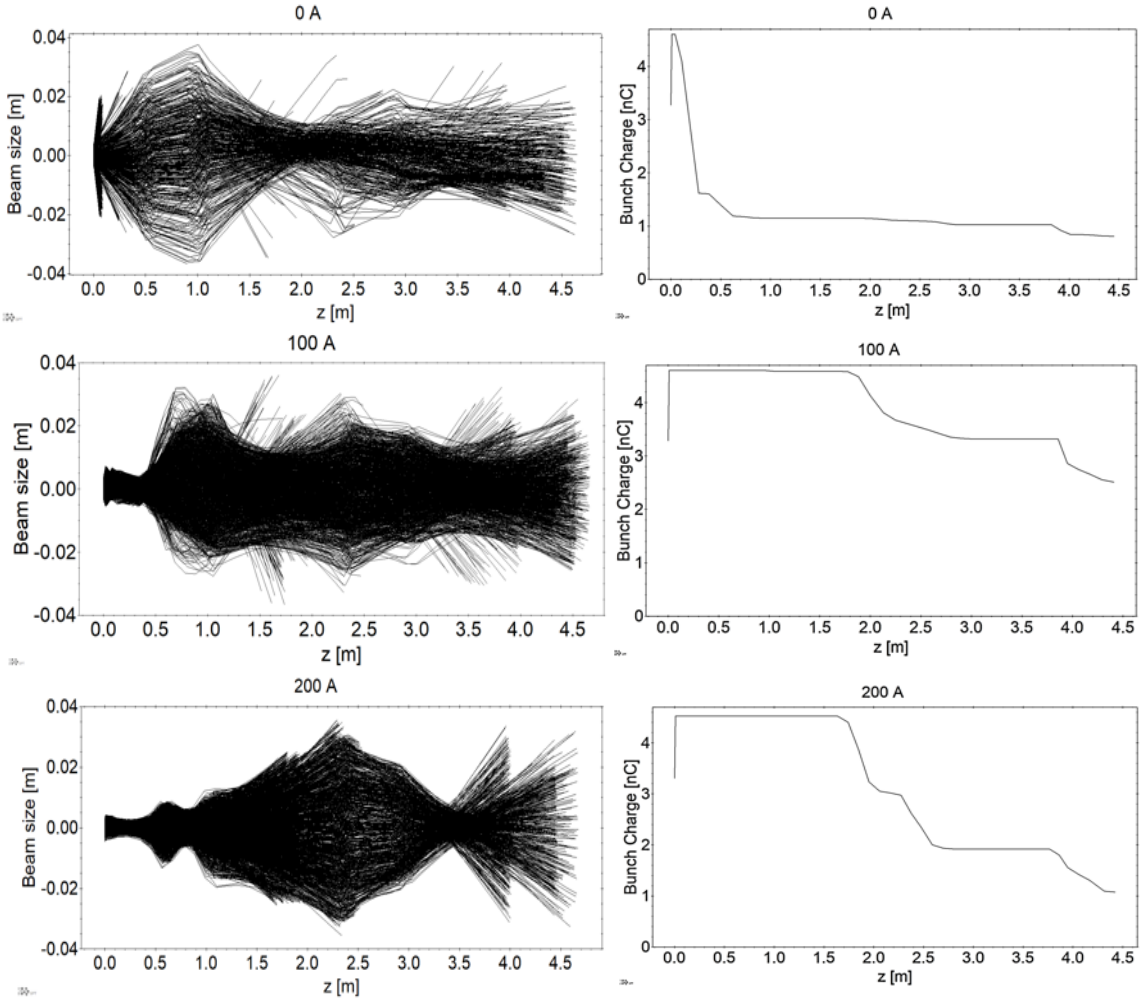

Beam Loss

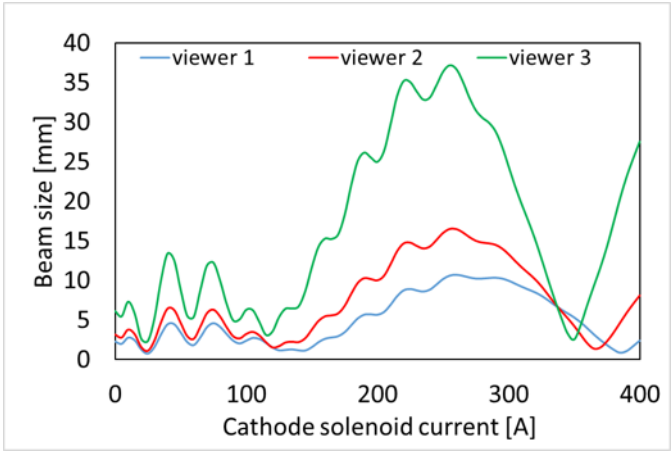

- Beam size varies with the gun solenoid current, thus the beam loss too

Characterization of space charge effect in magnetized beam cont'd

Space charge current limitation dependence on gun high voltage

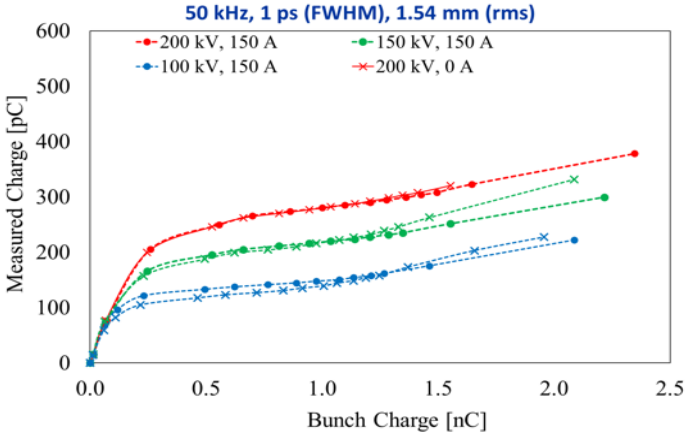

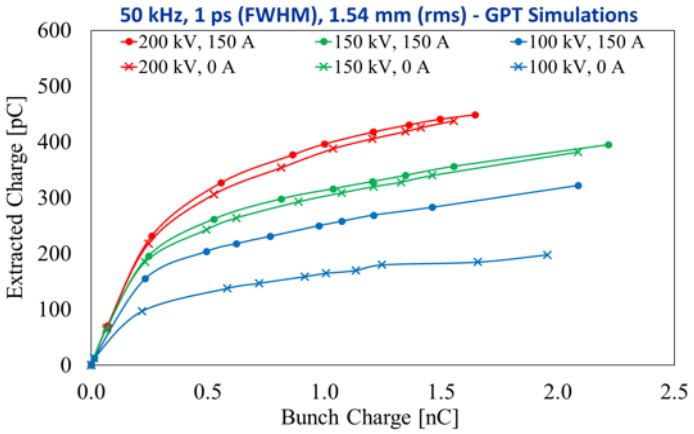

Space charge current limitation dependence on laser spot size

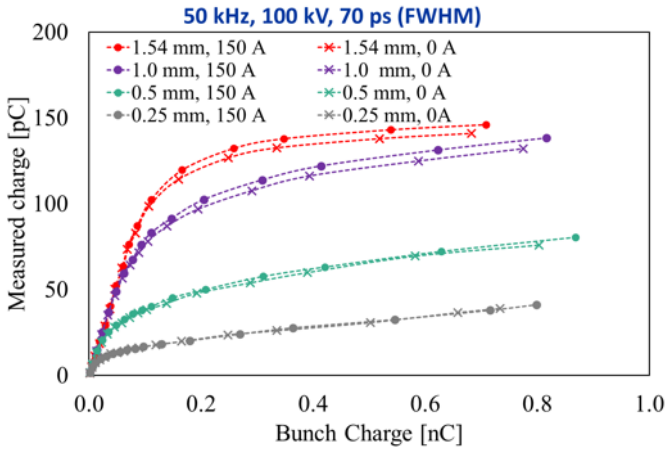

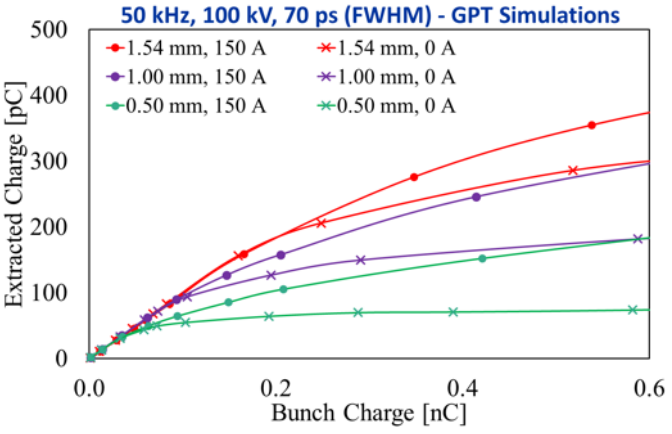

- Measured charge at the dump increase with the higher gun voltage, and larger laser spot size in the clean beam transport regime
- Less notable dependence on magnetization

Redesigning of the DC high voltage photogun

Motivation

- The accelerating electric field (E_z) at the photocathode sets the limit on the maximum charge density extractable from the photocathode
  - Current electric field at the cathode front is 2.5 MV/m which is relatively small for deliver nC bunched beam
  - Increase E_z at the cathode –by removing the Pierce geometry and decreasing anode-cathode gap
- Inverted insulator and triple point junction screening electrode, asymmetric NEG pumps combine in to introduce asymmetric electric fields in between the anode-cathode gap which then result in deflecting the beam vertically at the exit of the anode, difficulty in beam steering, and ultimately beam losses
  - Find a way to correct the beam deflection with minimum changes on the existing design
- Reliable operation at -300 kV high voltage with high quality beam and 10^{-12} Torr scale vacuum without field emission and high voltage breakdown.

Pierce focusing geometry 25°

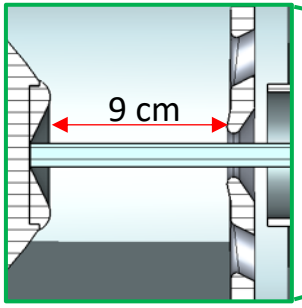

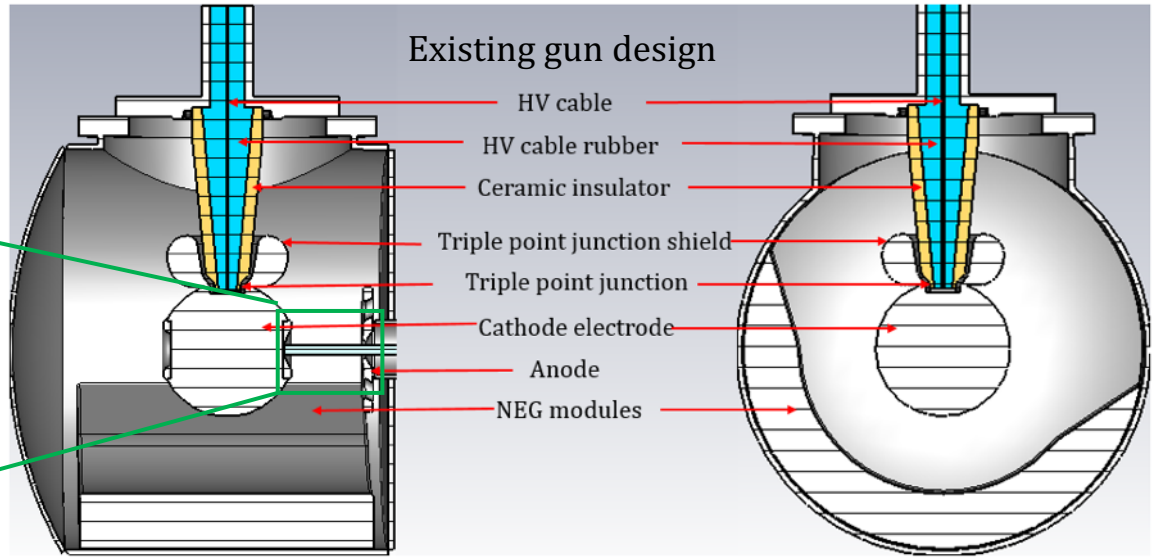

Redesigning of the DC high voltage photogun cont'd

Electrostatic design of the existing gun

-350 kV at the cathode, 0 V at the anode

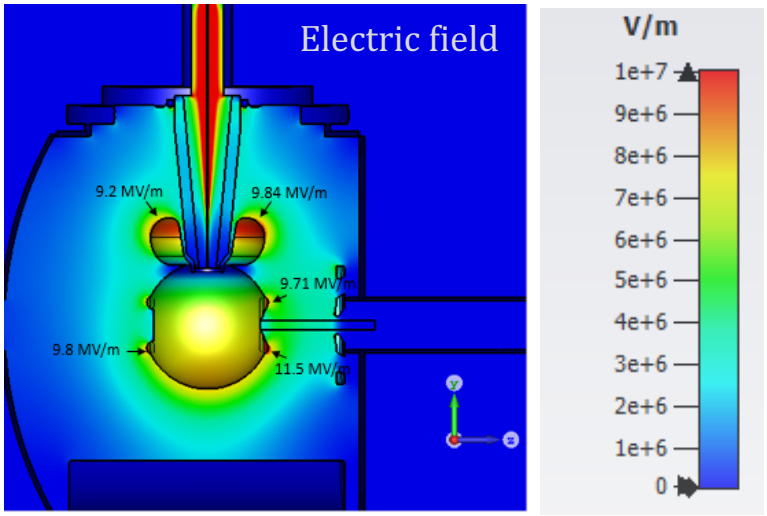

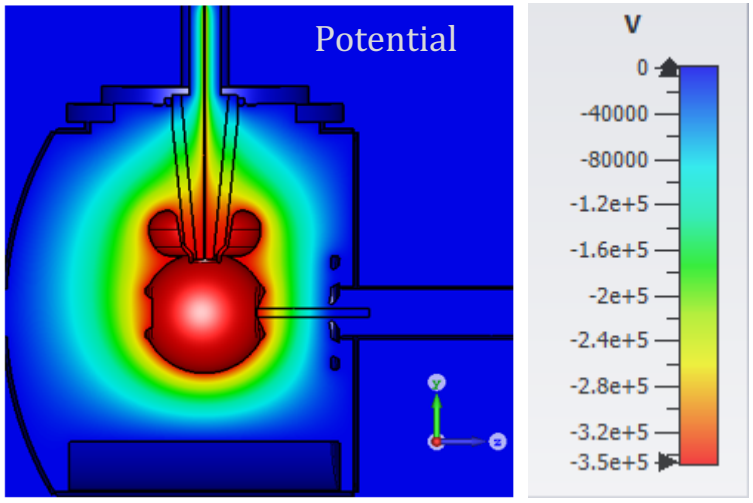

- To minimize field emission, to have long photocathode lifetime.
  - Optimize electrode shape (radius of curvature), size, and anode-cathode gap to have electric field $\leq$ -10 MV/m at -350 kV everywhere inside the chamber
  - Polished electrodes
  - High voltage conditioning
- To prevent high voltage insulator breakdown (i.e., arcing) an linearize the potential across the insulator
  - Design triple junction shield

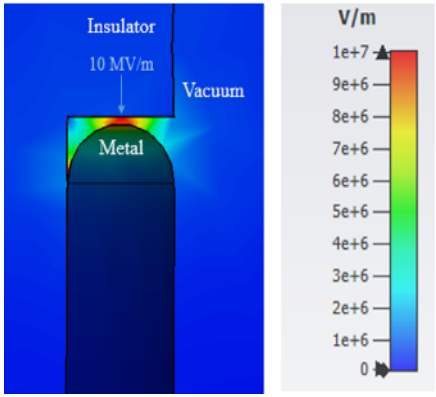

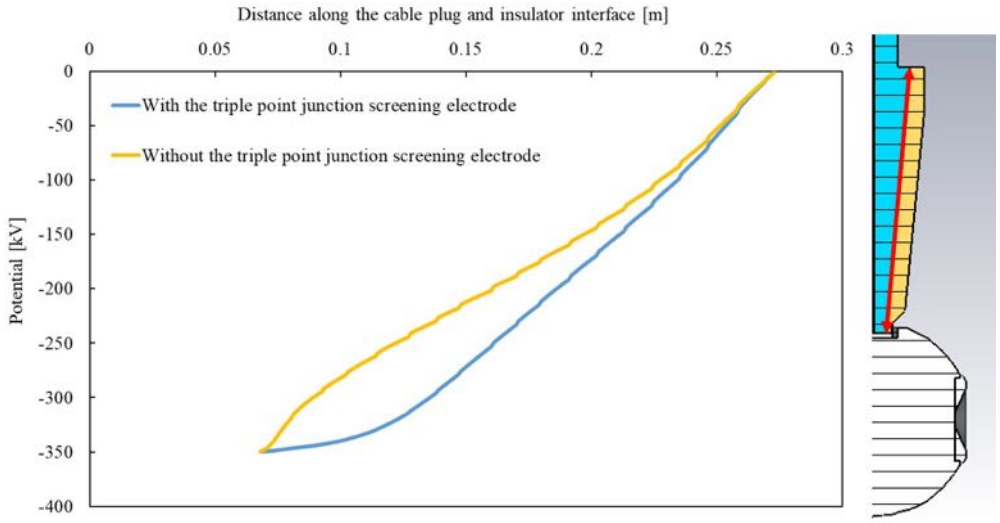

Redesigning of the DC high voltage photogun cont'd

Longitudinal electric field

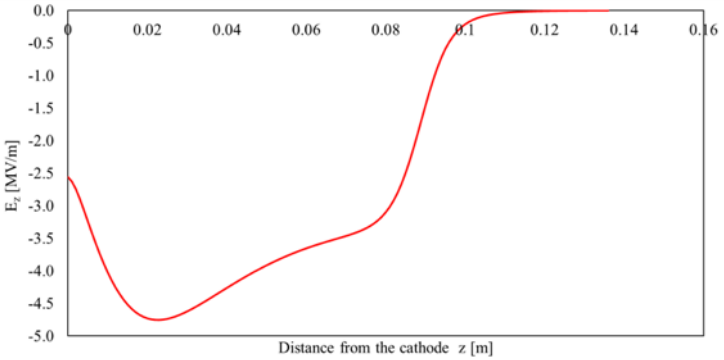

Horizontal electric field

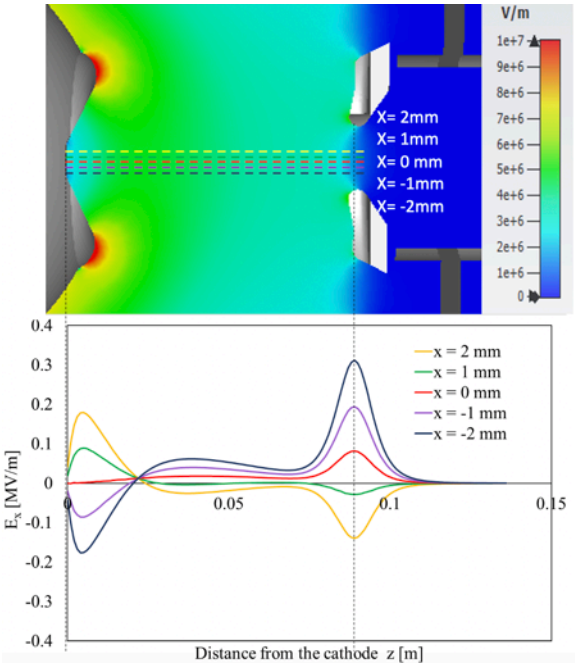

Vertical electric field

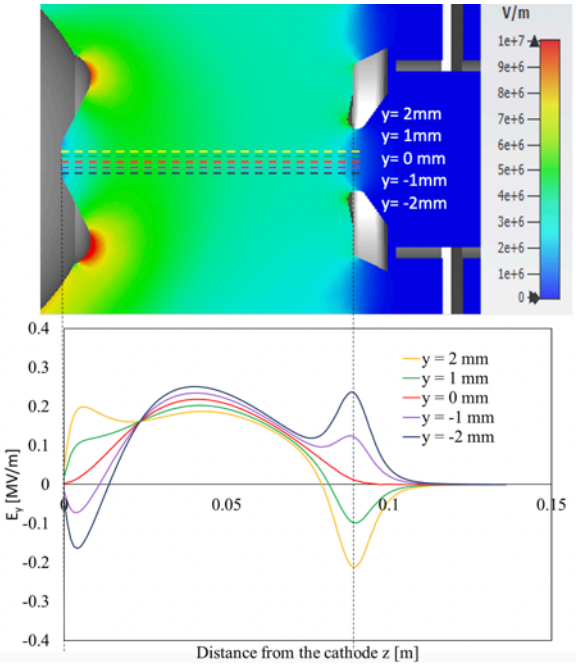

- The electric field at the cathode front is 2.5 MV/m
- E_z reached its maximum not at the cathode front but at 2 cm and E_x and E_y fields focused at the same position due to the Pierce geometry
- Asymmetry in E_x
  - Beam deflect 3 mm at z=1 m
  - Due to the asymmetry in placing the NEG pumps at the bottom of our gun chamber
- Huge asymmetry in E_y
  - Beam deflect 3.3 cm at z=1 m
  - Due to the inverted insulator and screening electrode

Beam deflection as a result of the asymmetric fields

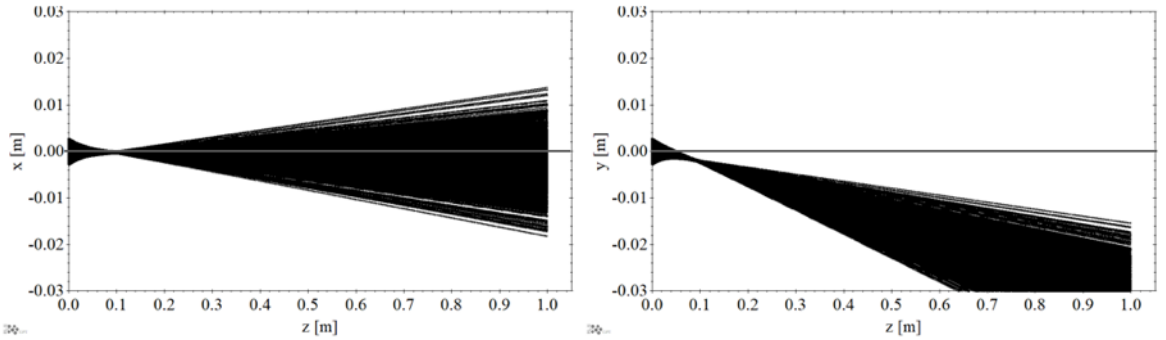

Redesigning of the DC high voltage photogun

Modified design

- To increase E_z at the cathode
  - Removed the Pierce geometry – flat cathode front and flat anode front
  - Reduced anode-cathode gap to 5 cm
- To correct the beam deflection with minimum changes on the existing design
  - Y deflection - Shift anode -1.6 mm in vertical direction
  - X deflection - Replace existing NEGs with thinner strips

Finalized mechanical design

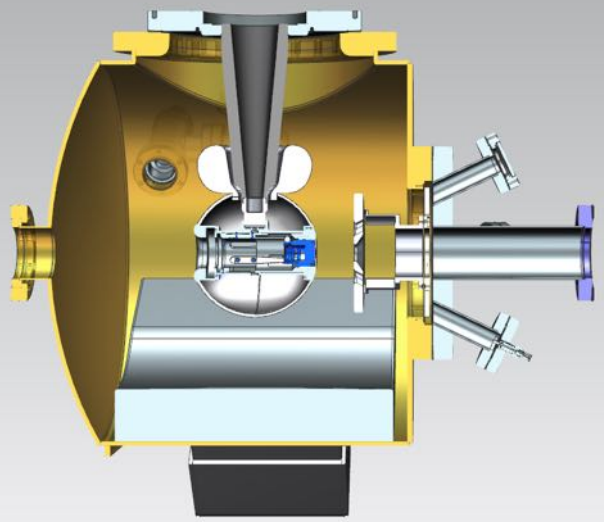

Modified gun design

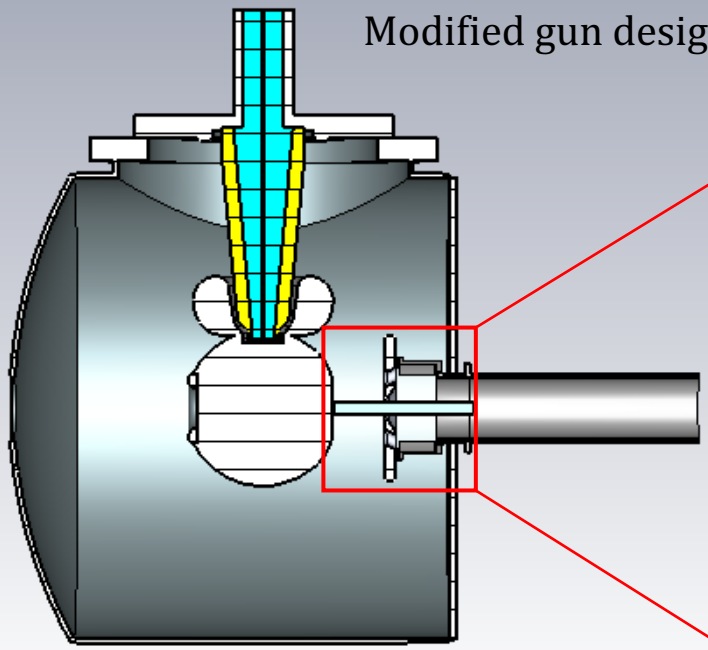

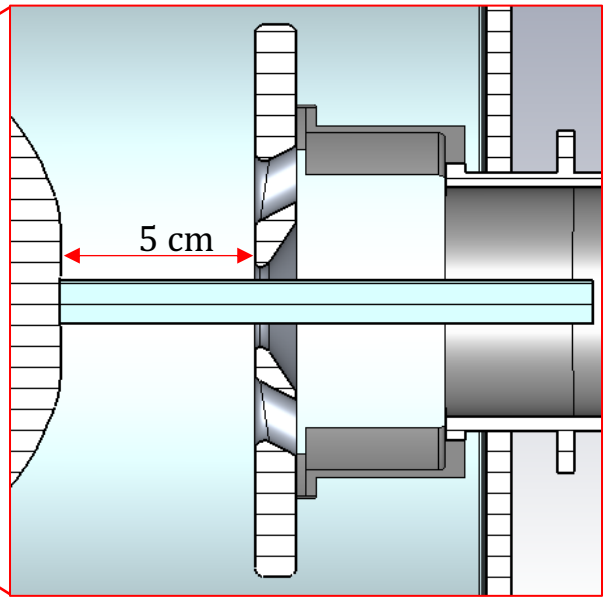

Anode mounting model

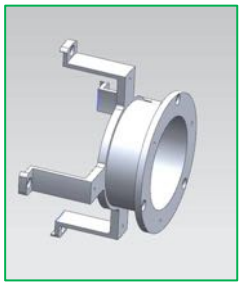

Redesigning of the DC high voltage photogun

Electrostatic design of the modified gun

-350 kV at the cathode, 0 V at the anode

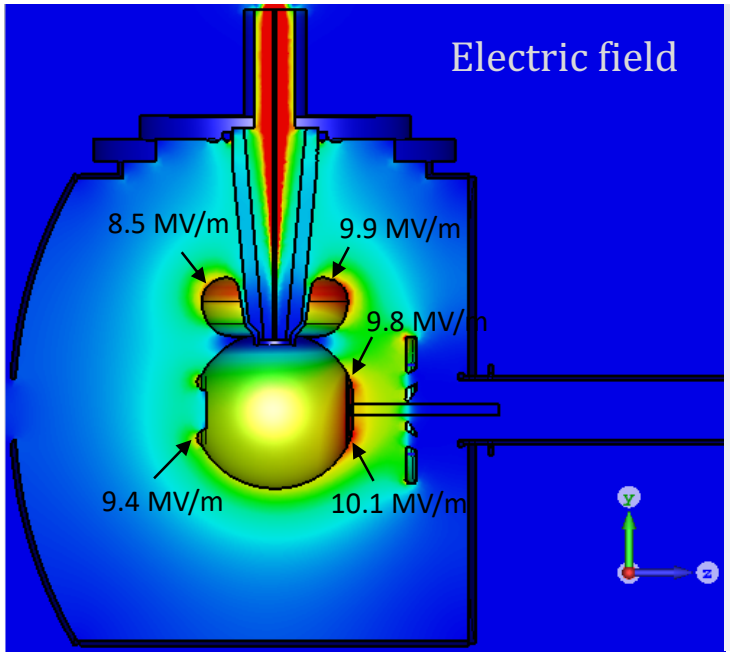

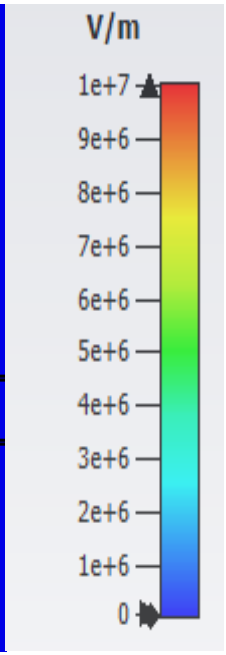

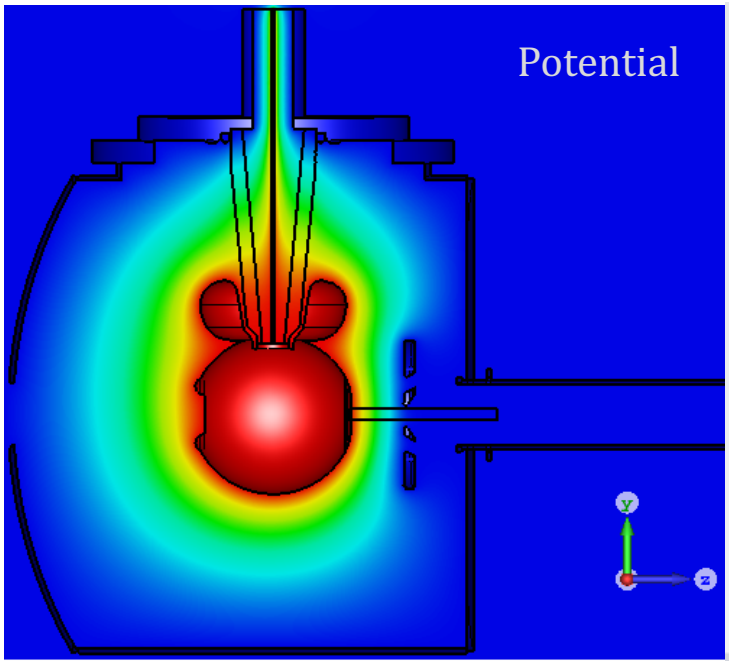

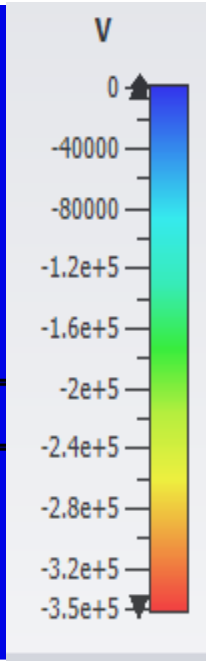

Longitudinal electric field

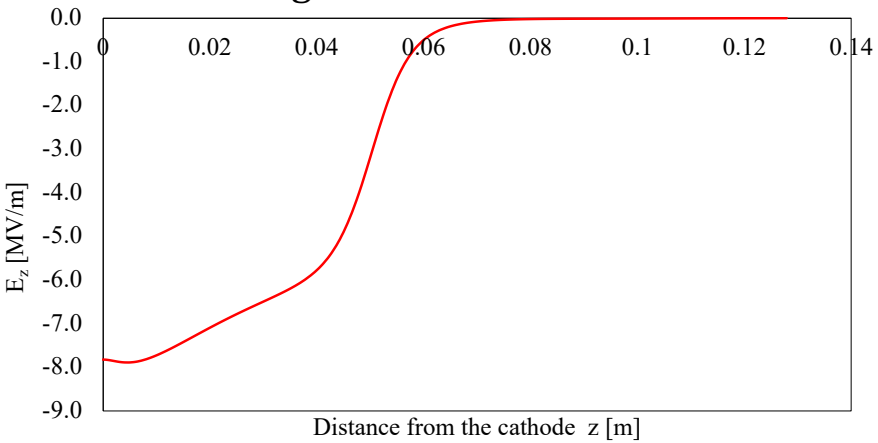

- The electric field at the cathode front increased to 7.82 MV/m from 2.5 MV/m

Redesigning of the DC high voltage photogun cont'd

Horizontal electric field

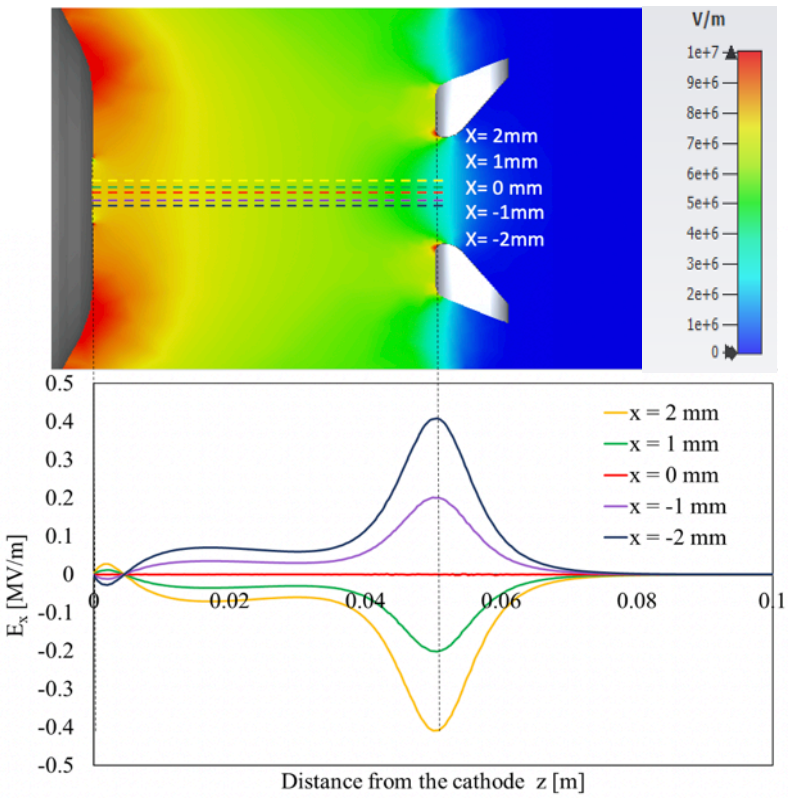

Vertical electric field

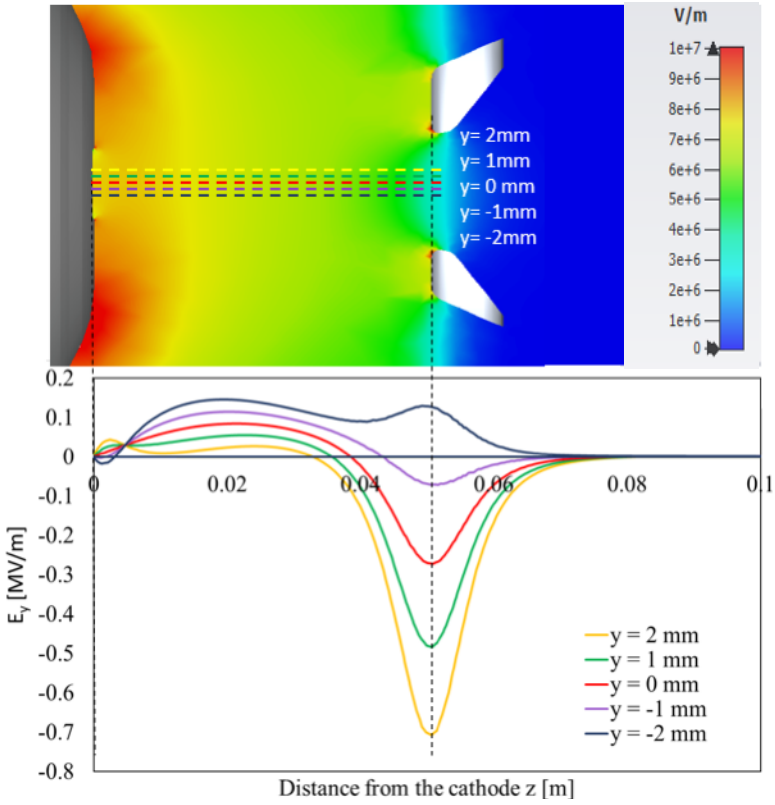

Beam trajectories with the new field maps

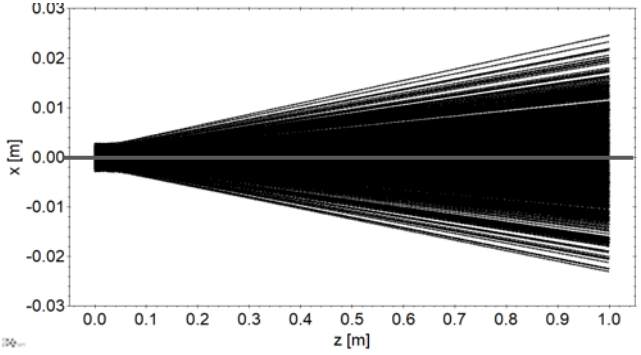

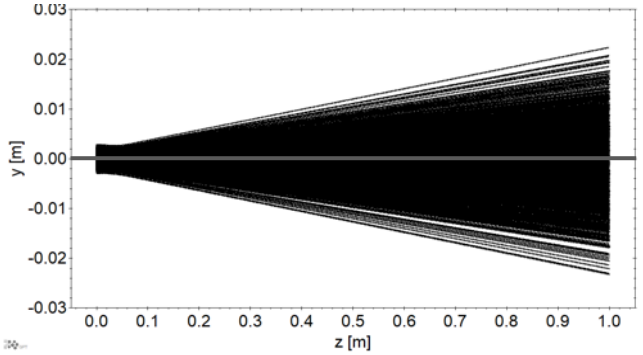

More GPT simulations with the modified photogun

Simulation parameters

Parameter	Value
Gun high voltage [kV]	-300
Magnetic field, B_z at the cathode [T] (0, 30, 180, 200 A)	0, 0.025, 0.15, 0.17
Mean Transverse Energy [eV]	0.130
Pulse width, Gaussian (FWHM) [ps]	75
Transverse laser spot size, Gaussian (rms) [mm]	1.64
Bunch charge [nC]	0.01 to 14
Horizontal offset of the laser [mm]	0
Vertical offset of the laser [mm]	0

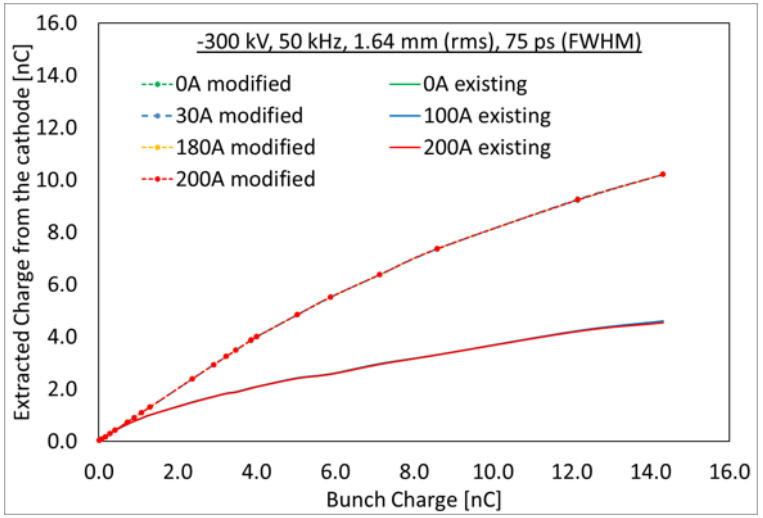

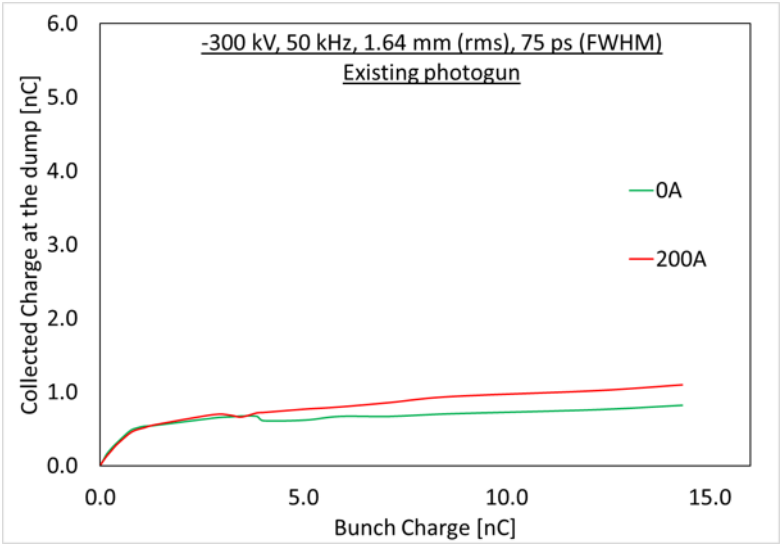

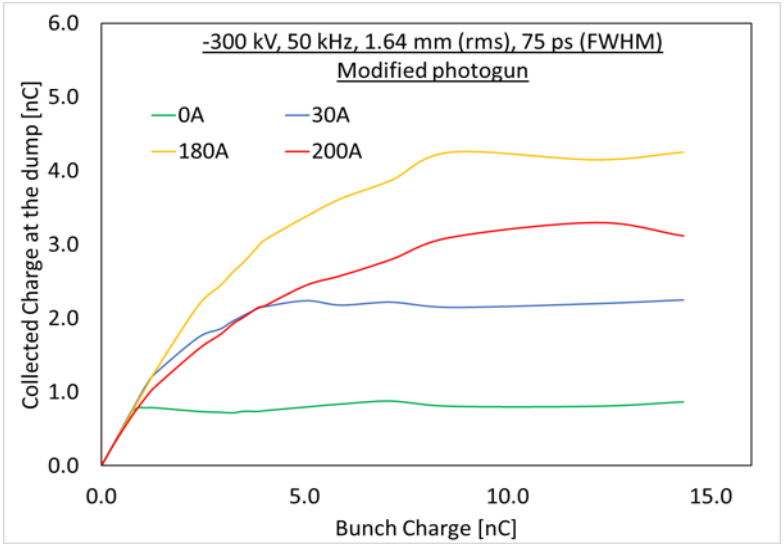

- Charge extracted from the cathode increased with the higher E_z
- According to simulations, charge extracted from the cathode does not depend on the magnetization
- Charge collected at the dump also increased with the higher E_z
- Charge collected at the dump critically affected by the beam loss, which depend on the beam sizes and hence the magnetization (mismatch oscillations)

GPT simulations with the modified photogun cont'd

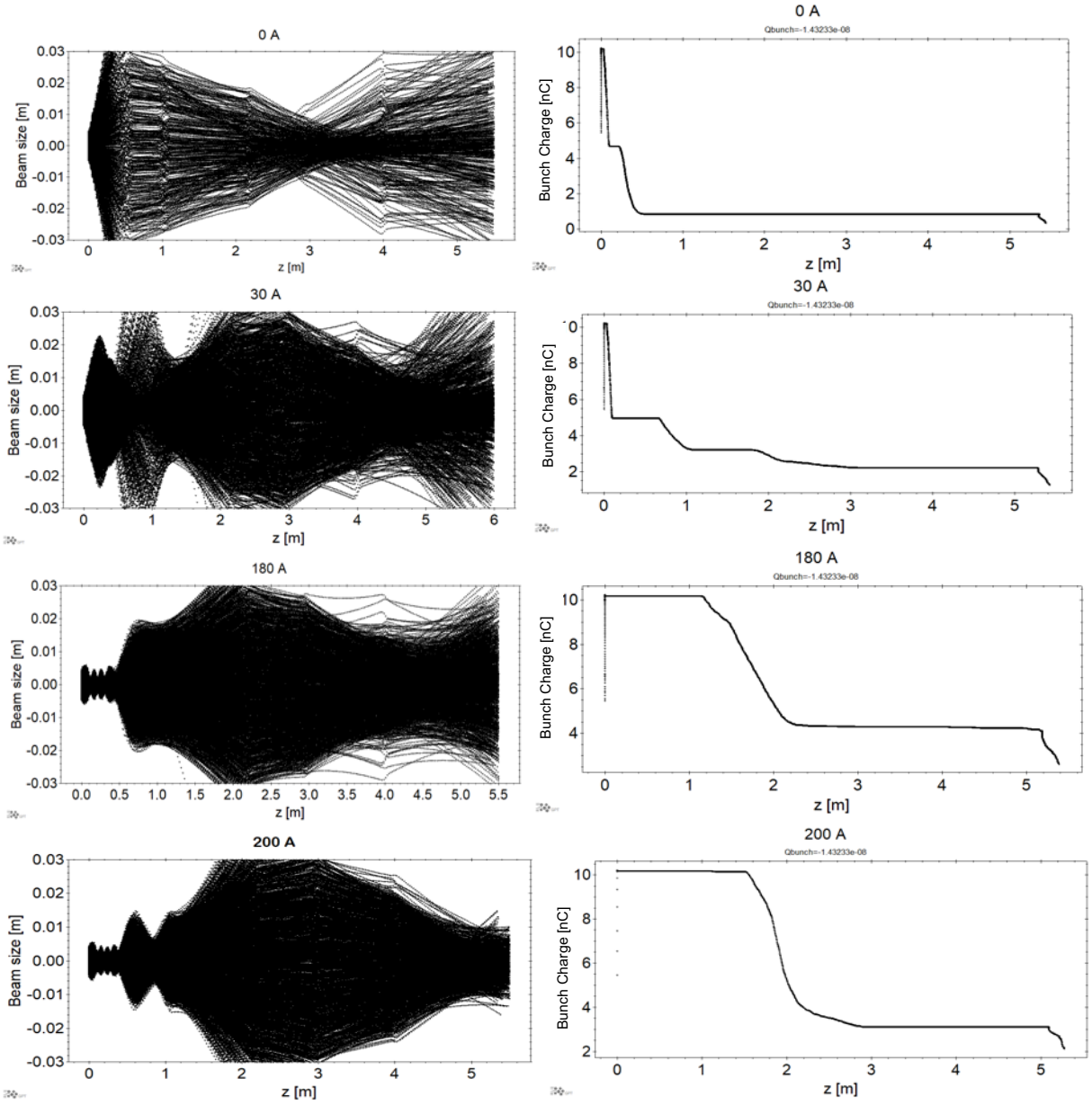

- Optimized the focusing solenoids to minimize the beam loss
- Modified the beamline by removing smaller radius components to reduce beam loss
- Did not use any corrector magnets as the beam is centered form the gun

Summary

- Magnetized beam was successfully generated from a -300 kV DC photogun, characterized with a modest diagnostic beamline and simulated using ASTRA and GPT software:
  - Studied beam size, rotation angle, and emittance variations as a function of applied magnetic field
  - Identified mismatch oscillation due to the non-uniform magnetic field hence the focusing of the beam in addition to the magnetization
  - Identified convergence of the beam results in negative rotation angles
- Investigated the space charge effect in magnetized electron beam and successfully simulated using GPT software.
  - Measurements were taken by varying the laser power and tracking the average current at the dump for different cathode solenoid currents
  - Demonstrated high bunch charge up to 700 pC
- Observations from measurement:
  - Not enough data to conclude space charge effect and space charge current limitation dependence on the magnetization
  - The space charge current limitations can be reduced by using a higher gun voltage with larger laser spot size at the cathode, regardless of the beam being magnetized
  - Lower accelerating field [E_z]at the cathode result in lower charge extraction
  - Beam loss due to limited beamline aperture and insufficient strength of the focusing solenoids plays a critical part in the measurements
- Observations from GPT simulation:
  - No notable dependence of the space charge current limitations on magnetization
  - Beam loss also depends on the magnetization strength as a result of mismatch oscillations

Summary cont'd

- Redesigned the photogun to increase E_z at the cathode while correcting the beam deflection cause by asymmetric fields
  - Increased E_z to 7.82 MV/m from 2.5 MV/m by removing the Pierce geometry and decreasing anode-cathode gap to 5 cm from 9 cm
  - Discovered a smart way to get rid of the beam deflection just by lowering the anode hole by 1.6 mm which will be implemented in CEBAF photogun
  - This will be a huge advantage for all the photogun to minimized the beam loss at the exit of the anode
- Simulated the beamline with modified photogun
  - Charge extracted form the cathode doubled with the modified gun
  - Charge collected at the dump also increased with higher E_z
- Planning to repeat the measurements on space charge dominated beam with the modified photogun, a new laser, and a new photocathode for a more thorough study

To-do list

- Photogun work: total estimated time 3-4 months

  •Finalize the mechanical design of the new components of the gun COMPLETE
    - Anode mounting - finalized the spider model COMPLETE
    - Puck/puck holding design for flat cathode front COMPLETE

  •Making the new electrodes machine shop work (some pieces have been made) 4 weeks
    - Ball cathode front face
    - Anode & anode mount
    - Puck holder

  •Barrel polishing & UHV cleaning: 1 week

  •Gun assembly: 4 weeks
    - Remove existing electrode, anode, NEG pumps :1 week
    - Re-connect gun to beam line and replace existing NEG with thinner strips :1 week
    - Assemble new anode in gun vacuum chamber : 0.5 weeks
    - Assemble new electrode in clean room :1 week
    - Final gun assembly :0.5 weeks

  •Vacuum bake out: 1.5 weeks

  •High voltage conditioning with Kr: 2-3 weeks
    - For gun solenoid on and off

- Laser work: 2 weeks
- Photocathode fabrication: 2 weeks
- Initial beamline commissioning: 2 weeks

To-do list cont'd

- Take measurements: total estimated time 3-4 weeks
  - Measure extracted charge at the dump by increasing laser power for different magnetization strengths
  - Measure extracted charge at the dump by increasing laser power for different magnetization strengths by changing voltages, laser pulse widths, laser spot sizes
  - Find a way to measure correlated and uncorrelated emittance
  - Add Faraday cup ~ 2 m to track the beam loss

- Simulations
  - Write a code to calculate correlated and uncorrelated emittance for space charge dominated beam
  - Simulate all the measurements

- Thesis writing: total estimated time 4-5 months

- Paper writing
  - Magnetized beam generation and characterization
  - On modified photogun
  - On space charge effect in magnetized beam

Graduation (Hopefully) : May-Aug 2021

References

[1]. W. Herr and B. Muratori. Concept of Luminosity. Yellow Report CERN 2006-002.
[2]. G. I. Budker. Atomnaya Energiya, 22(346), 1967.
[3]. Y. Derbenev. Theory of electron cooling. 1978.
[4]. Ya. Derbenev and A. Skrinsky. Magnetization effect in electron cooling. Sov. J. Plasma Phys, 4:492, 1978.
[5]. Reiser. Theory and Design of Charged Particle Beams. 2008.
[6]. Ya Derbenev Y. Zhang H. Zhang, D. Douglas. Electron cooling study for meic. Proceedings of the 6th International Particle Accelerator Conference, Richmond,VA, 6, 2015.
[7]. D. L. Bruhwiler V. N. Litvinenko A. V. Fedotov, I. Ben-Zvi and A. O. Sidorin. High-energy electron cooling in a collider. New J. Phys, 8:283, 2006.
[8]. Ya. Derbenev. A method to overcome space charge at injection. AIP Conf. Proc, 14, 2006.
[9]. K.-J. Kim N. Barov S. Lidia J. Santucci R. Tikhoplav J. Wennerberg Y.-E Sun, P. Piot. Generation of angular-momentum-dominated electron beams from a photoinjectory. Phys. Rev. ST Accel. Beams, 7, 2004.
[10]. M.A. Mamun et al. Production of magnetized electron beam from a dc high voltage photogun. Proceedings of IPAC2018, Vancouver, Canada, 2018.
[11]. M. Migliorati M. Ferrario and L. Palumbo. Space charge effects. Proceedings of the CAS- CERN Accelerator School,Geneva, 2014.
[12]. I. Langmuir. The effect of space charge and residual gases on thermionic currents in high vacuum. Phys. Rev. 2, pages 450–486, 1913.
[13]. J. P. Verboncoeur Y. Feng. Transition from fowler-nordheim field emission to space charge limited current density. Phys. Plasmas 13., 2006.
[14]. Ya. Derbenev. A method to overcome space charge at injection. AIP Conf. Proc., 2005.
[15]. M.J. de Loos S.B. van der Geer. General Particle Tracer User manual.
[17] P. Adderley, J. Clark, Joe Grames, John Hansknecht, K. Surles-Law, D. Machie, M. Poelker, M. Stutzman, and Rau Suleiman. Load-locked dc high voltage gas photogun with an inverted-geometry ceramic insulator. Phys. Rev. ST Accel. Beams, 13:10101, 12 2009.
[18]. C. Hernandez-Garcia et al., Compact 300 kv dc inverted insulator photogun with biased anode and alkali-antimonide photocathode. Phys. Rev. ST Accel. Beams, page 22, 2019.
[19]. C. Hernandez-Garcia M. Poelker G. Palacios-Serrano, F. Hannon and H. Baumgart. Electrostatic design and conditioning of a triple point junction shield for a 200 kv dchigh voltage photogun. Rev. Sci. Instrum., page 89, 2018.

THANK YOU !

Jefferson Lab

Old Dominion University

U.S. Department of Energy | Office of Science

JSA

Back up slides

Importance of the magnetized electron beam

Electron cooling

- Invented by G.I. Budker in 1965 for the purpose of increasing luminosity of hadron collider.

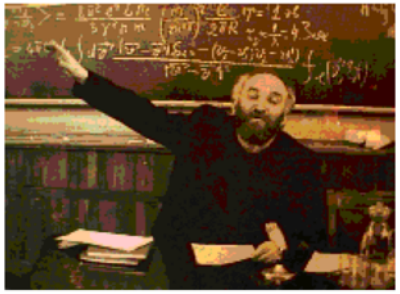

- It was first tested in Novosibirsk in 1974 with 68 MeV protons at NAP-M storage ring, which had cooling length of 1 m.

- The idea behind this is when a “cold” electron beam co-propagated with the “hot” ion beam with same velocity, Coulomb collisions between ions and electrons lead to a transfer of thermal motion from ions to the electrons, in a similar way that two gasses in a mixture reach thermal equilibrium.

- Thus, electron cooling reduces the spread in the longitudinal and transverse ion velocities, which means a decrease in the momentum spread, in the diameter, and in the divergence of the ion beam.

Emittance compensation in a magnetization beam

Emittance

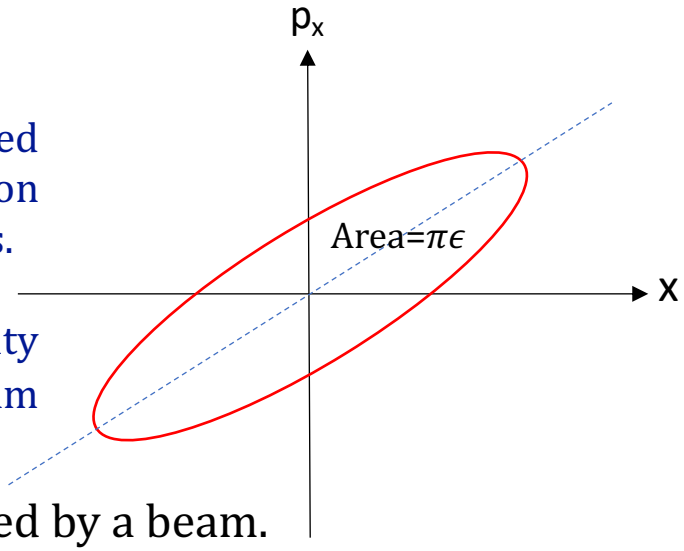

- The motion of charged particles in a beam can be described completely by six degrees of freedom in *phase space:* position (x, y, z) and momentum (px , py , pz) in Cartesian coordinates.
- This concept is very powerful in beam dynamics as, the density of particles in phase space does not change along a beam transport line: Liouville's theorem.
- Emittance is a measure of the phase space area occupied by a beam.

$$\int_{ellipse} dx\, dp_x = \pi\epsilon$$

rms emittance: $\epsilon_{rms} = \sqrt{\langle x^2\rangle\langle {p_x}^2\rangle - \langle x p_x\rangle^2}$

Normalized rms emittance: $\epsilon_{n,rms} = \frac{1}{m_0 c}\sqrt{\langle x^2\rangle\langle {p_x}^2\rangle - \langle x p_x\rangle^2}$

Geometric emittance : $\epsilon_{rms} = \frac{m_0 c}{\langle p_z\rangle}\epsilon_{n,rms}$ ➡ $\epsilon_{n,rms} = \gamma\beta\,\epsilon_{rms}$

Thermal emittance: $\epsilon_{n,th} = \sigma_0\sqrt{\frac{kT}{m_0 c^2}}$, T cathode temperature , σ_0 rms beam size at the cathode

Beam size $=\sqrt{\epsilon_{rms}\beta}$, β-beta function